doi:10.1093/brain/awn087 *Brain* (2008), **131**, 1783–1792

Intra-cortical connectivity in multiple sclerosis: a neurophysiological approach

Franca Tecchio,[1,2] Giancarlo Zito,[2,3] Filippo Zappasodi,[1,3] Maria Luisa Dell'Acqua,[4] Doriana Landi,[4] Davide Nardo,[3] Domenico Lupoi,[3] Paolo M. Rossini[2,3,4] and Maria M. Filippi[3]

[1]Istituto Scienze e Tecnologie della Cognizione—CNR, Unità MEG, Roma, [2]Casa di Cura San Raffaele Cassino e IRCCS San Raffaele Pisana, [3]Dipartimento di Neuroscienze ed Unità Operativa Complessa Radiologia Diagnostica ed Interventistica, AFaR, Ospedale Fatebenefratelli and [4]Neurologia Clinica, Universitá Campus Biomedico, Roma, Italy

Correspondence to: Dr ssa Franca Tecchio, Unità MEG, Dipartimento di Neuroscienze, Ospedale Fatebenefratelli, Isola Tiberina, 00186 Rome, Italy
E-mail: franca.tecchio@istc.cnr.it

Multiple sclerosis is an autoimmune disease predominantly affecting the white matter of the CNS, causing—among functional sequelae—cortico-cortical partial or total disconnection. Since functional connectivity linking cerebral regions is reliably reflected by synchronization of their neuronal firing, in this study an electrophysiological parameter measured by magnetoencephalography was used to quantify an intra-cortical connectivity (ICC) index focused on the primary somatosensory cortical areas (SI). Twenty-one patients affected by mild (Extended Disability Scale Score, median 1,5) relapsing-remitting (RR) multiple sclerosis in the remitting phase without clinically evident sensory impairment were evaluated. Three dimensional MRI was used to quantify the lesion load, discriminating black hole and non-black hole portions, normalized by individual brain volumes. When matched with a control population, multiple sclerosis patients showed a reduced ICC combined with the complete loss of the finger-dependent functional specialization in SI cortex of the dominant hemisphere. No association was found between ICC impairment and disease duration, or prolongation of the central sensory conduction time, presence of spinal cord lesions and ongoing disease modifying therapy. The ICC index slightly correlated with the lesion load. A local index of ICC in a circumscribed brain primary area was altered in mildly disabled RR-multiple sclerosis patients, also in absence of any impairment of central sensory conduction. In conclusion, the diffuse damage influencing the multi-nodal network subtending complex cerebral functions also affects intrinsic cortical connectivity. The SI ICC index is proposed as a highly sensitive and simple-to-test functional measure for the evaluation of intra-cortical synchronization mechanisms in RR-multiple sclerosis.

Keywords: magnetoencephalography; cerebral connectivity; primary sensorimotor cortex; lesion load black holes

Abbreviations: BHV = black hole volume; CCT = central conduction time; EDSS = Extended Disability Scale Score; EEG = electroencephalography; FSS = functional source separation; ICC = intra-cortical connectivity; LrF = lesion relative fraction; MEG = magnetoencephalography; PD = proton density; SI = primary somatosensory cortical areas; RR = relapsing-remitting; TLV = total lesion volume; WMHy = white matter hyperintensities

Received December 3, 2007. Revised April 11, 2008. Accepted April 15, 2008. Advance Access publication May 23, 2008

Introduction

Multiple sclerosis is an autoimmune disorder characterized by multiple lesions of the central myelin and accumulating clinical signs due to demyelination and progressive axonal damage (Keegan and Noseworthy, 2002). As a consequence of white matter injury, a partial or total disconnection from subcortical and spinal targets occurs, in parallel with deficits of cortico-cortical connectivity. Current efforts are devoted to delineating brain connectivity changes from an anatomical perspective through MRI techniques such as voxel-based morphometry and diffusion tensor imaging-based fibre tracking (Cercignani *et al.*, 2002; Audoin *et al.*, 2007; Cader *et al.*, 2007; Reich *et al.*, 2007). However, such techniques only provide information on anatomical substrates mainly related to contingents of large, unidirectional fibres. Blood oxygen level-dependent functional MRI, assessing alterations of neural activations in brain diseases including multiple sclerosis, has been enriched with

functional and effective connectivity algorithms to more directly characterize neural connectivity impairments (Leocani and Comi, 1999; Reddy *et al.*, 2000; Horwitz, 2003; Au Duong *et al.*, 2005; Horwitz *et al.*, 2005; Audoin *et al.*, 2006; Cader *et al.*, 2006). Such an approach does not allow investigation of rapid (millisecond range) phenomena linked with transient increments/decrements of neural assembly activities and functional cortico-cortical connectivity. In fact, studies in animals and humans demonstrate that separate cerebral regions synchronize their neuronal firings when functionally connecting each other (Gray *et al.*, 1989; Engel *et al.*, 2001; Fellous *et al.*, 2001). Electro- and magneto-encephalography (EEG and MEG, Del Gratta *et al.*, 2001) represent non-invasive neurophysiological techniques with appropriate temporal resolution to detect such phenomena in humans. Previous EEG coherence data in progressive multiple sclerosis patients demonstrated a significant decrease of alpha and theta band coherence between both anteroposterior and inter-hemispheric areas correlated with cognitive impairment and subcortical lesion load on MRI (Leocani *et al.*, 2000). Likewise, a decreased alpha band inter-hemispheric coherence was found by Cover and colleagues (2006) in relapsing-remitting (RR) multiple sclerosis patients through a MEG paradigm.

Our group has previously identified a MEG synchronization measure within the primary sensory hand cortical area (S1) showing finger-dependent functional specialization in the dominant hemisphere of right handed healthy subjects (Tecchio *et al.*, 2007*a*). In fact, the thumb cortical representation, activated in response to a sensory stimulus, is more phase locked than the little finger representation. These phase-locking phenomena reflect activity in S1 cortex sensitive to the strength of cortico-cortical connections and, therefore, provide an intra-cortical connectivity index (ICC).

The aim of the present study was to test whether the ICC index measured in S1 is involved in a cohort of patients affected by RR-multiple sclerosis. In order to assess the test sensitivity, we purposefully selected patients with absent or minimal disability in remitting phase and without clinically evident sensory deficits at the time of evaluation. Particular care was also devoted to a precise quantification of the lesion-load. Three-dimensional high resolution anatomical images were coregistered with lesion sensitive images estimating white matter hyperintensities (WMHy). We focused on the relationship between the ICC and putative MRI markers of axonal loss (black holes), because they appear to correlate more closely to the development of multiple sclerosis disability than traditional MRI features (Truyen *et al.*, 1996; Bitsch *et al.*, 2001).

Patients and Methods

Patients

Patients were recruited on the basis of the following inclusion criteria: diagnosis of multiple sclerosis according to McDonald *et al.*'s Criteria (2001); RR clinical course (Lublin and Reingold, 1996); low degree of disability as estimated by Extended Disability Scale Score (EDSS, Kurtzke, 1983) $<3{,}5$; absence of clinical relapse or radiological evidence of disease activity for at least 3 months preceding the study; absence of sensory symptoms at the moment of recruitment; no treatment with corticosteroids or psychotropic drugs within the previous 3 months.

The study was approved by Ethic Committee of 'S. Giovanni Calibita' Hospital and all patients gave written consent.

Clinical, neurophysiological and neuroradiological examination

In addition to EDSS, upper limb sensory evoked potentials were collected and the central conduction time (CCT) calculated following standardized methods and criteria (Mauguière *et al.*, 1999). All patients underwent cervical and brain MRI examination at least 6 months before and at the time of recruitment.

MRI exam

MR image acquisition. Imaging was performed at the Radiology Unit, equipped with an Achieva 1.5 T scanner (Philips Medical Systems, Best, The Netherlands), provided of 33 mT/m gradient amplitude, online 2D/3D geometric distortion correction and a standard quadrature head coil. The acquisition protocol consisted of one 3D high resolution anatomical sequence and a group of four 2D sequences for lesion characterization. The former was empirically optimized to increase grey/white matter image contrast (T1-weighted Turbo Field Echo TR/TE/FA = 9.5 ms/4 ms/8°; 256^2 matrix, 160 coronal contiguous slice, in-plane resolution 0.98 × 0.98 mm). The latter included a dual spin echo (TR/TE/FA of, respectively, 4000 ms/20–120 ms/90°, yielding to a T2 and a proton density—PD—weighted images); two T1-Spin Echo sequences (TR/TE/FA of, respectively, 550 ms/15 ms/60°, one before intravenous injection of the contrast agent gadolinium and the second 5 min later) and one FLAIR (TR/TE/FA = 10 000 ms/100 ms/90°). All 2D sequences were acquired as axial oblique contiguous 3 mm slices (256^2 image matrix, 240 mm field of view), encompassing the bi-commisural plane. After entering the PACS system of the Department, the DICOM images were post-processed on a dual processor Linux workstation. All subjects underwent an identical imaging protocol. The MRI scanner did not undergo major hardware upgrades during data collection.

MR image analysis (lesion characterization, optimized segmentation and volumes calculation for normalization). The high resolution 3D anatomical images were coregistered to the PD/T2 dataset in order to exactly match the regions of the brain in which an abnormal signal intensity could be detected by a trained neuroradiologist.

A region of interest's approach was used to manually trace the regions that showed abnormal signal intensity, either as hyper- or hypo-intensity, according to the visual inspection. MRICro software (Brett *et al.*, 2001) allowed the delineation of such regions classified as being white matter PD/T2 hyperintensities (WMHy). Within the WMHy regions, the black hole areas, identified as pre-contrast T1 persistently hypo-intense and coincident T2 hyper-intense lesions, were submitted to a separate measurement (Fig. 1). According to post-contrast behaviour, black holes are divided into 'acute' black holes if showing gadolinium enhancement (Matthews, 1999; van Waesberghe *et al.*, 1999) and 'permanent'

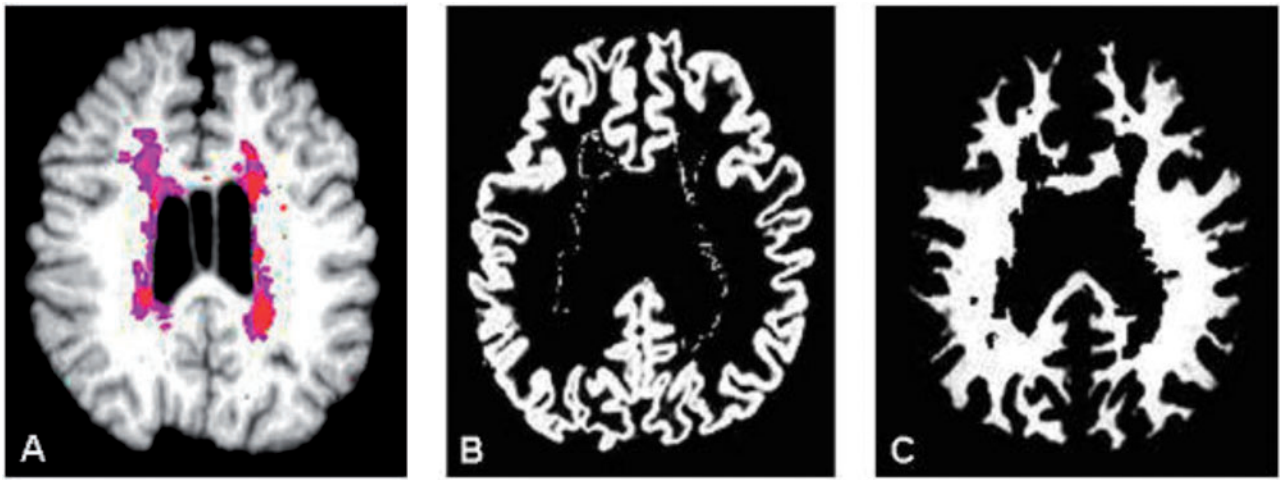

Fig. 1 MRI analysis. Brain T1-3D MRI in a representative patient (**A**) the whole parenchyma is shown with the total amount of lesions, classified in non-black hole (nBH; purple) and black hole (BH) portions (red). Gray matter (**B**) and normal appearing white matter (**C**) volumes are segmented from T1-FLAIR coregistered brain images to normalize all brain fractions in Talairach space, after lesion removal to minimize the possibility of misclassification artefacts. Slices **B** and **C** correspond to z-coordinate = 28.

black holes if not, while being detectable on a previous MRI session performed at least 6 months earlier (Bagnato *et al*., 2003).

To correctly normalize the lesion volume in each patient, procedures aimed at identifying the intra-cranial structures were carried out. The lesional region of interest's where then subtracted from the 3D anatomical images, yielding to 3D lesion-free images that entered an optimized segmentation process. Statistical parametric mapping software (SPM2, www.fil.ion.ucl.ac.uk/spm, Friston *et al*., 1995) running under MATLAB 7.2 (the Mathworks, Inc., MA, USA) was used to manually reorient each subject's dataset, pointing the origin to the anterior commissure. To improve the accuracy of segmentation, a preliminary iterative normalization/segmentation procedure was performed on the 3D lesion-free images, as implemented in optimized voxel-based morphometry method (Good *et al*., 2001). A study-specific template was created for several reasons: (i) minimizing potential normalization problems related to differences of registration to the standard space among patients' brains; (ii) to take into account the demographics of our patients, who had a frequent involvement of periventricular and *corona radiata* white matter and (iii) to reduce the magnetic field inhomogeneities and non-uniformities related to the static magnetic field. The normalization matrices derived from previously obtained lesion-free volumes were applied to their own lesional region of interest images, resampled to $1 \times 1 \times 1$ mm for anatomical accuracy. The overall lesion-specific volumes were calculated firstly as number of voxels within each image, then transformed into millilitres.

MRI variables. Three MRI variables were considered that characterized the lesion load:

- the total lesion volume (TLV), i.e. the volume of the whole T2 WMHy;
- the black hole volume (BHV);
- the volume of the non-black hole portion of the total lesion (nBHV = TLV−BHV).

These three quantities were divided by the standardized normalization factors, i.e. total white matter and the brain parenchyma with and without the cerebrospinal fluid (for nomenclature see Table 1).

Table 1 Nomenclature of lesion load normalized factors

	Normalization factors		
	WMV	BPV	TIV
TLV	LrF	LpF	LF
BHV	BHrF	BHpF	BHF
nBHV	nBHrF	nBHpF	nBHF

Nomenclature used for the different normalization factors, obtained by dividing the TLV = total lesion volume, BHV = black holes volume and nBHV = volume of the non-black hole portion of the total lesion by the total white matter volume (WMV, first column), the total brain parenchyma volume (BPV, second column) and the total intra-cranial volume (TIV, third column).

Functional ICC exam

Recordings. MEG data were separately acquired during the electrical stimulation of the thumb and little finger of the right and left hand (ring electrodes, 0.2 ms electric pulses, inter-stimulus interval of 641 ms, stimulus intensities set at about twice the subjective somatosensory threshold) and compared with the rest state. Recordings were carried out via a 28-channel system operating in a magnetically shielded room (Vacuumschmelze Gmbh), the active channels being evenly distributed on a spherical surface (13.5 cm of curvature radius) and covering a total area of about 180 cm^2. Cerebral activity from rolandic areas have been recorded via a single position on the hemisphere contralateral to the stimulated hand, by centring the recording apparatus on the C3/C4 positions of the 10–20 international EEG system. MEG data were sampled at 1000 Hz (pre-sampling analogical filter 0.48–256 Hz), and collected for off-line processing.

ICC index. By submitting MEG signals to the procedure called functional source separation (FSS, Tecchio *et al.*, 2007*b*), the source activities of cortical neural networks devoted to the contralateral thumb and little finger sensory perception were segregated in each hemisphere. FSS comes from the blind source separation algorithms, which separate sources, exploiting their own signal waveform, while remaining blind to their biophysical relationships with the recorded signal (Cichocki and Amari, 2002). The aim of FSS is to enhance the separation of relevant signals by exploiting some *a priori* knowledge without renouncing the advantages of using only information contained in original signal waveforms. In fact, starting from an independent component analysis model, FSS identifies a source on the basis of its functional behaviour. In addition to the identified functional source (FS) time signal (FS(t)), the field distribution it generates can be obtained by retro-projecting the source activity in the space scanned by the MEG sensors, being thus used as the input for inverse-problem solution algorithms. In the present study, FS(t) related to the thumb ($FS_T(t)$) and little finger ($FS_L(t)$) cortical representations were identified by requiring maximal responsiveness at around 24 ms to the corresponding contralateral finger stimulation (Barbati *et al.*, 2006). It is well known that this latency marks the primary sensory area (S1) response to specific projections coming from thalamus after hand fingers stimulation. Moreover, MEG is sensitive to the field generated by pyramidal neurons tangentially oriented to the scalp, i.e. topographically positioned within the walls of cortical sulci. The identified sources (FS_T and FS_L) are thus localized in the post-central wall of the Rolandic sulcus in the area 3b, as demonstrated by Barbati and colleagues (2006). Once identified the time signals $FS_T(t)$ and $FS_L(t)$, they were considered as two mutually interconnected portions of the hand representation in sensory area, as previously observed that FS_T responded also to the little finger stimulation—with around half the strength than when stimulating the thumb—and vice versa for FS_L (Barbati *et al.*, 2006). The sensory cortical connectivity was estimated as the phase locking between these source activities. Connectivity of the thumb sensory cortical representation was obtained as the phase locking after the stimulation of the thumb (ICC_T). The same was done for the little finger representation ICC_L (Tecchio *et al.*, 2007*a*, see Appendix I). In right handed healthy subjects (mean age ± SD: 31 ± 8 years, 7 females and 7 males, Edinburgh Inventory Test Score > 85) the ICC in the dominant hemisphere demonstrated somatotopic properties. In fact, ICC_T was higher than ICC_L. Moreover, both ICC_T and ICC_L were correlated with the contralateral finger sensorimotor dexterity (Tecchio *et al.*, 2007*a*), as quantitatively estimated by the 'fingertip writing' test (Lezak, 1976). The cited study documented that all these properties were evident selectively in the gamma frequency range [(33, 45)Hz].

Statistical analysis

ICC_T and ICC_L value distributions did not differ from a Gaussian (Kolmogorov-Smirnov $P > 0.400$).

The ICC of the network devoted to S1 representation of the thumb (ICC_T) and of the little finger (ICC_L) were studied by a repeated measure analysis of variance with *Hemisphere* (left, right) and *Finger Representation* (thumb, little finger) as within-subject factors and *Group* (controls, multiple sclerosis patients) as the between-subject factor. Factors of interest were *Group*, indicating different ICC properties in healthy subjects and patients, as well as the interaction factor *Finger Representation* × *Group* indicating alterations of the physiological somatotopy of the index in patients.

For those electrophysiological measures, which were different in patients from in controls (significance threshold $P < 0.05$), possible bivariate correlations with the clinical and neuroradiological measures were carried out. Since neuroradiological variable distributions differed from a Gaussian (consistently, Kolmogorov Smirnov test, $P < 0.054$), non-parametric tests were applied.

Patients' and controls' group age distributions did not differ from Gaussian (Kolmogorov-Smirnov $P > 0.400$ for both). The two group ages did not differ (independent sample t-test $P > 0.400$). No dependence on age was observed in the control group for any of the ICC index (Pearson $P > 0.200$ consistently). No effect of gender was present on any ICC index, as indicated by the between-subject factor *Gender* [$F(1,10) = 0.006$, $P = 0.941$] in the analysis of variance design, together with the absence of significance of any interaction effect with intra-subject factors *Hemisphere* (left, right) and *Finger Representation* (thumb, little finger).

Results

Patients

Twenty-one right-handed (Edinburgh Inventory > 85, Oldfield, 1971) RR-multiple sclerosis patients with a low degree of disability (median EDSS 1, 5; Table 2) were enrolled. They presented a mean disease duration of 10 ± 7 years and a median relapse rate of 0.33 (Table 2). Ten patients were on therapy with interferon-β-1a.

Although 13 out of the 21 patients claimed upper or lower limb sensory symptoms in the past (11 upper limb—4 of whom bilateral—2 lower limb), none of them presented any of this at the time of MEG evaluation in agreement with the inclusion criteria. Nine patients of the

Table 2 Clinical and radiological characteristics of patients

Mean Age, years (SD)	40 (8)
Sex (M : F)	5 : 16
Median EDSS (5–95 percentiles]	1.5 (0–3.5)
Mean disease duration, years (SD)	10 (7)
Median relapse rate (5–95 percentiles)	0.33 (0.08–2.23)
Disease modifying therapy, number of patients	10
History of cervical lesions, number of patients	15
Prior right arm sensory symptoms, number of patients	9
Prior left arm sensory symptoms, number of patients	6
CCT right arm prolongation, number of patients	9
CCT left arm prolongation, number of patients	10
Median LrF, ml (5–95 percentiles)	0.047 (0.001–0.208)
Median BHrF, ml (5–95 percentiles)	0.010 (0–0.038)
Median nBHrF, ml (5–95 percentiles)	0.037 (0–0.017)

Four patients suffered from bilateral arm sensory symptoms. Nine patients had bilateral CCT prolongation. EDSS = Extended Disability Scale Score; CCT = central conduction time; LrF = lesion relative fraction; BHrF = black hole relative fraction; nBHrF = non-black hole relative fraction.

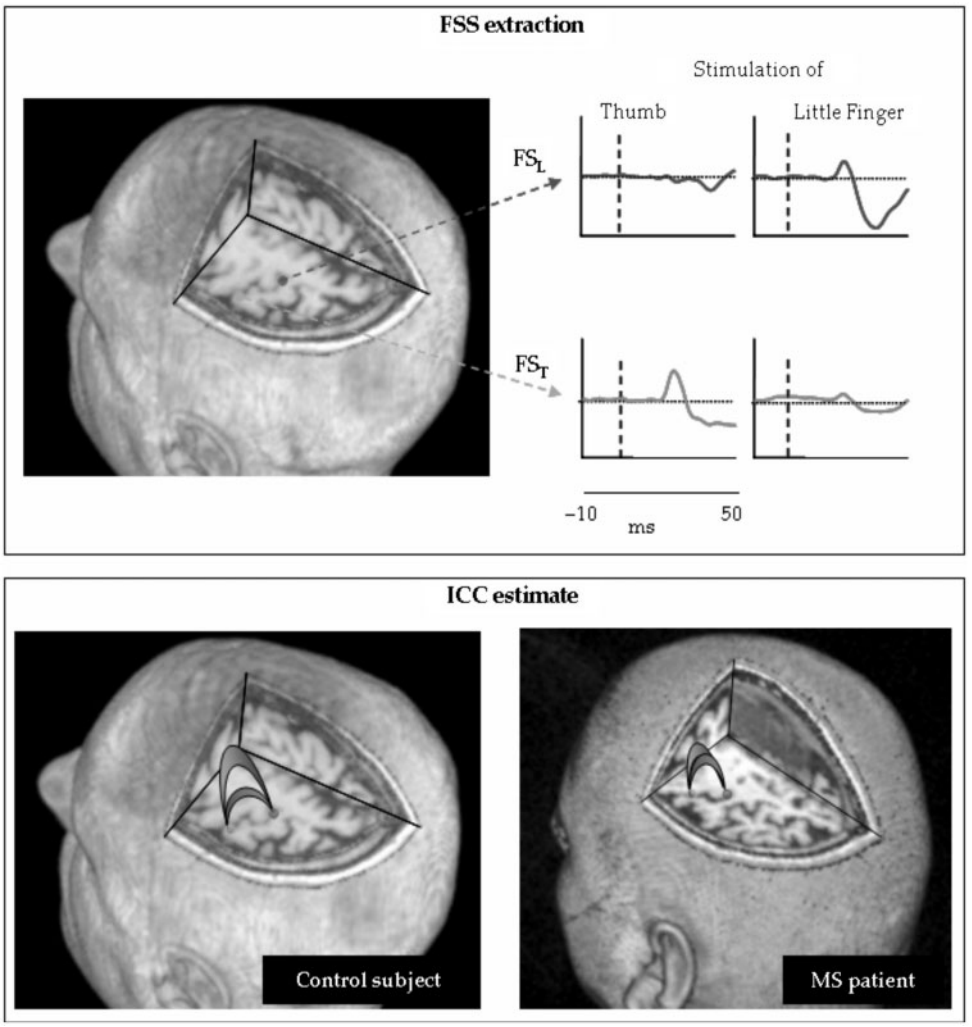

Fig. 2 FS_T and FS_L behaviour and ICC. In one representative subject top left, topographical representation on a 3D reconstructed brain volume of the extracted sources representing the thumb (FS_T) and the little finger (FS_L) central primary representations projected on a suitable axial plane centrally located with respect to the two sources. Top right, dynamics of FS_T and FS_L activities during contra-lateral thumb and little finger stimulation, shown after averaging the source signal timed on the stimulus onset ($t = 0$, vertical line) in the [−10, 50] ms time window. Bottom, the gamma band phase locking, i.e. the ICC index, of the right thumb (green) and little finger (light blue) representation. Note that in the multiple sclerosis patient, the finger-dependent functional specialization (thumb > little finger, Tecchio *et al*. 2007*a*) is lost.

11 with prior upper limb sensory symptoms showed delayed latency of scalp potentials with a normal cervical potential and prolonged CCT (Table 2).

Fifteen patients had a positive history of one or more cervical plaques, seven of whom still showed the lesions at the recruitment time (Table 2).

In agreement with the inclusion criteria of being in remitting phase, no patient had acute black holes (stable black hole behaviour in the two MRI exams performed at least 6 months apart one each other). No grey matter lesions were detected in 19 of our patients and very few millimetric lesions at cortical or juxtacortical level of frontal lobes and at the vertex were present in two patients. Normalized lesion fractions with respect to the total white matter volume are provided in Table 2.

Functional ICC

Since ICC_T and ICC_L behaved differently in the right and left hemispheres [*Hemisphere* × *Finger Representation* interaction factor $F(1,29) = 6.086$, $P = 0.020$, Fig. 3], separate investigations were carried out. In the right hemisphere, ICC_T and ICC_L considered together were lower in patients than in controls [*Group* factor $F(1,31) = 4.189$, $P = 0.049$, Fig. 2]. Neither ICC_T or ICC_L differed in the two groups when compared separately ($P > 0.200$ consistently). In the left hemisphere, the clear distinction between thumb and little finger representations, observed in healthy subjects, was lost in patients [*Finger Representation* × *Group* interaction factor $F(1,29) = 11.915$, $P = 0.002$, Fig. 3]. In fact, while in controls ICC_T was greater than ICC_L (paired *t*-test $P = 0.001$), ICC_T and ICC_L values did not differ in multiple sclerosis

patients ($P = 0.354$; Fig. 3). Moreover, in the left hemisphere mean ICC_T was smaller in patients than in controls (Fig. 3, Independent sample *t*-test, $P = 0.047$). No difference between the two groups was found for ICC_L ($P = 0.228$). As a consequence, left hemisphere ICC_T was studied in relationship with the clinical and neuroradiological findings. To assess whether the ICC reduction was due to reduced responsiveness from primary area, the strength of the M20 equivalent current dipole (Barbati *et al.* 2006) activated in response to the thumb and little finger was compared in patients and controls. The analysis of variance model with *Finger* as within-subject factor and *Group* as between-subject factor, indicated no significance of differences in patients and controls [$F(1,21) = 1.364$, $P = 0.256$].

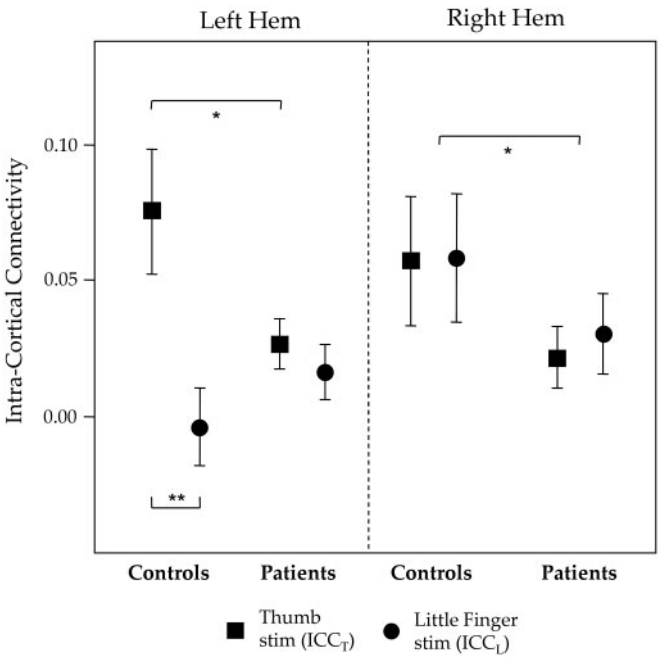

Fig. 3 ICC in healthy and multiple sclerosis patients. ICC in the two hemispheres and for the thumb (ICC_T) and little finger cortical representations (ICC_L) in healthy subjects and multiple sclerosis patients. In the right hemisphere, both ICC_T and ICC_L were smaller in patients than in healthy subjects. In the left hemisphere, the ICC somatotopy ($ICC_T > ICC_L$) was lost in patients, and ICC_T was smaller in multiple sclerosis patients than in controls.

Relationship among left hemispheric ICC_T, clinical, neurophysiological and radiological state

The ICC_T was not associated to right median nerve central sensory conduction time prolongation: in fact, similar ICCT values were equally found in patients with normal and increased CCT [paired *t*-test $t(17) = 0.206$, $P = 0.839$]. Neither ICC_T was modified by the occurrence of a cervical lesion in the clinical history [independent sample *t*-test $t(18) = -1.708$, $P = 0.105$]. No association was present between ICC_T and either EDSS (Spearman's rho $P = 0.410$, or disease duration ($P = 0.958$, Fig. 4) or history of sensory symptoms [independent *t*-test $t(19) = -0.430$, $P = 0.671$]. Moreover, in those patients with very long disease duration ($\geqslant 10$ years, nine patients) with the present low EDSS values, suggesting a benign form, no difference of the ICC_T value was found with respect to the other patients [independent sample *t*-test $t(19) = 1.430$, $P = 0.170$]. No association linked ICC_T and relapses rate (Pearson' r $P = 0.966$). Interferon therapy had no relationship with ICC_T values (independent samples *t*-test $P = 0.709$).

A slightly inverse correlation was found between the ICC_T and the lesion relative fraction (LrF) (Table 3). Further investigating this relationship, two patients' subgroups could be identified according to the extent of LrF

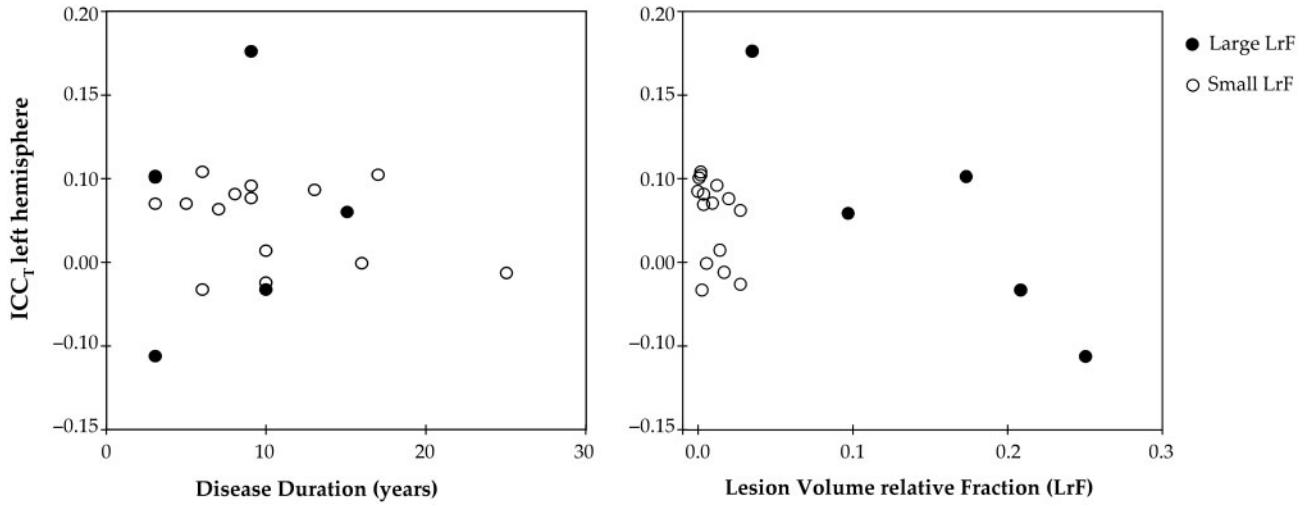

Fig. 4 ICC_T versus disease duration and lesion load. Scatter plot of left hemisphere ICC_T with respect to the disease duration (left) and the lesion relative fraction (LrF, right). Two distinct subgroups are differentiated by smaller and larger TLVs.

Table 3 Left ICC_T — lesion load correlation

	Left hemispheric ICC_T		
	Total ($n = 20$)	LrF < 0.03 ($n = 15$)	LrF ⩾ 0.03 ($n = 5$)
LrF	−0.408 (0.075)	−0.579 (0.024)	−0.900 (0.037)
BHrF	−0.253 (0.281)	−0.304 (0.271)	−0.100 (0.873)
NBHrF	−0.405 (0.077)	−0.575 (0.025)	−0.900 (0.037)

Spearman's correlations rho (*P*-values) between intra-cortical connectivity of the right thumb representation network (ICC_T) in the left hemisphere and the lesion load, including the total = LrF lesion relative fraction and the BHrF = separate black hole relative fraction, and nBHrF = non-black hole relative fractions. The subgroup of patients with higher lesion is small, and the result is not reliable.

(Fig. 4). The inverse correlation was confirmed even in patients with smaller lesion volumes (Table 3). Moreover, in this subgroup, the ICC_T value tended to decrease with respect to the healthy subjects [independent *t*-test for equal variances not assumed $t(14.068) = 1.871$, $P = 0.082$].

To understand whether a different role is played by black hole and non-black hole lesion portions, their correlation with the ICC_T was considered separately. We found that the association was present with non-black hole relative fractions and not with black hole relative fractions (Table 3). The black hole relative fraction was slightly smaller than the non-black hole relative fraction [paired *t*-test $t(20) = -2.568$, $P = 0.018$].

Discussion

An altered pattern of ICC with a significant reduction of ICC index within primary sensory areas in multiple sclerosis patients with low or minimal disability was found. ICC did not associate to the clinical state, probably as a consequence of the homogeneity of EDSS toward lower scores. ICC was independent of any prolongation or delay of CCT or the radiological evidence of spinal lesions. No reduction of S1 cortical responsiveness was documented in patients. These findings support the idea of a mainly cortical origin of the alteration. Furthermore, the finger-dependent functional specialization of hand sensorimotor network in the left hemisphere was lost in patients. In fact, while in healthy subjects the ICC of primary neural networks devoted to the thumb was higher than those related to the little finger, this pattern vanished in multiple sclerosis patients.

It is worth remembering that by ICC the level of connection between specific neuronal pools in the primary hand sensory region (area 3b) is tested by measuring the level of synchronization of their oscillating activities in the gamma band. Within cortical areas, the intrinsic functional connectivity measured by ICC stands on the anatomical topology of lateral connections, modulated by extrinsic inputs, whose architecture embodies specific predictions that have been acquired and stored during evolution and through experience-dependent learning (Hebb, 1949; Riehle *et al.*, 2000; von Stein *et al.*, 2000; Petersen and Sakmann, 2001; Lutzenberger *et al.*, 2002; Kaiser and Lutzenberger, 2005). Previous findings showed that the ICC index is possibly sensitive to the shaping of the lateral connections of the cortical 'modules' affected by dynamic learning processes. In fact in healthy subjects the ICC of both thumb and little finger primary sensory cortical networks correlated with contralateral finger *dexterity*, a parameter related to a sensorimotor perception skill (Tecchio *et al.*, 2007*b*). The relationship between high gamma band phase locking and the dexterity of the represented finger came out in the dominant hemisphere and not in the non-dominant one. This fits the modelling proposed by the 'temporal binding' theory of perception (Singer, 1999). This theory defines neural synchrony as crucial to enhance the saliency of neural responses. Our findings in healthy subjects indicate that the synchrony mechanisms become 'structural' of the network devoted to the most dexterous district. On these bases, the dynamic gamma band phase locking measured by ICC is suggested as a code for finger dexterity, in addition to the magnification of somatotopic central maps. Sensory perception relies on an anatomical hierarchy of neural networks made of synaptic relays—nodes—recruited by a feed-forward information flow, modulated by inter-nodal feed-back (Singer, 1999; Engel *et al.*, 2001; Varela *et al.*, 2001). Present results of reduced S1 ICC in patients could be understood in light of previous findings showing that within a multi-modal neural network, the disruption of connection fibres yields to changes of activation properties in single nodes (for a review Steriade, 2004). Differently from previous electrophysiological methods characterizing long-range anteroposterior and inter-hemispheric connectivity in multiple sclerosis (Leocani *et al.*, 2000; Cover *et al.*, 2006; for a review see Hoffmann, 2007), the ICC index is an innovative approach providing information about local ICC within a single primary area. The privileged role of S1, main origin of projections to primary motor cortex (Rizzolatti and Luppino, 2001), makes this node a 'second-last' station of almost all complex network processing. This hierarchical key role of S1, together with possible node activity impairments induced by inter-nodes' disconnections, suggests S1 ICC as a valuable marker of multiple sclerosis disconnection damage.

The slight inverse correlation between ICC and lesion load, in absence of any detectable S1 lesion, indicates a contribution of WMHy to ICC alteration. On the other hand, significant ICC reduction in patients, only slightly associated to the lesion load, can be viewed as a result of the widespread (cortical and subcortical) damage in multiple sclerosis, whose extent is more strictly associated to the clinical manifestations of the disease than the extent of focal pathology (for review see Barkhof, 2002; De Stefano *et al.*, 2002; Filippi and Rocca, 2005). An alternative hypothesis behind ICC alteration in patients could be that it is an epiphenomenon of circumscribed S1 cortical damage

below the level of lesion load analysis. The documented unaltered responsiveness of the thumb and little finger primary sensory areas indicates that possible S1 lesions do not alter the activation of the same neuronal pools whose interconnections are measured by ICC. These findings, thus, speak against the hypothesis of ICC reduction due to local lesions not detectable by our anatomical data assessment.

The slight inverse ICC correlation with the lesion load was more evident with non-black hole than with black hole portions. A hypothesis could be drawn that the ICC is more affected by non-black hole-mediated aberrant inputs than by impoverished inputs carried on by fibres bordering functionally idle black hole areas. Minimal load of both non-black hole and black hole areas in our patients, makes mandatory confirmations on patients' cohorts characterized by a wider range of lesion load.

In a previous study on RR-multiple sclerosis patients it was suggested that in the relapse phase of multiple sclerosis there is a cortical disinhibition possibly as compensation counteracting the damage in the course of the disease. In the remitting phase normal cortical excitability was observed (Caramia *et al.*, 1991, 2004). The extent and excitability of the recruited neuronal pool do not affect the ICC index, which only accounts for the level of intra-node connectivity, and was altered even in the remitting phase. S1 ICC estimate, if supported by correlation with clinical data in larger population follow-up studies, might represent an innovative index for functional evaluation in multiple sclerosis.

In our cohort of mildly affected patients, there seems to be little, if any, correlation between clinical and neuroradiological pictures and MEG results. Moreover, patients with rather short disease duration presented with the same ICC alteration pattern as patients with long disease duration. These findings suggest that the S1 connectivity impairment could be a functional marker of the presence of the disease.

In conclusion, an altered pattern of ICC within primary sensory areas in multiple sclerosis patients with low disability was found. S1 ICC estimate is proposed as a non-invasive index for functional connectivity loss in RR-multiple sclerosis.

References

Audoin B, Au Duong MV, Malikova I, Confort-Gouny S, Ibarrola D, Cozzone PJ, et al. Functional magnetic resonance imaging and cognition at the very early stage of MS. J Neurol Sci 2006; 245: 87–91.

Audoin B, Guye M, Reuter F, Au Duong MV, Confort-Gouny S, Malikova I, et al. Structure of WM bundles constituting the working memory system in early multiple sclerosis: a quantitative DTI tractography study. Neuroimage 2007; 36: 1324–30.

Audoin B, Ibarrola D, Ranjeva JP, Confort-Gouny S, Malikova I, Ali-Chérif A, et al. Compensatory cortical activation observed by fMRI during a cognitive task at the earliest stage of MS. Hum Brain Mapp 2003; 20: 51–8.

Au Duong MV, Boulanouar K, Audoin B, Treseras S, Ibarrola D, Malikova I, et al. Modulation of effective connectivity inside the working memory network in patients at the earliest stage of multiple sclerosis. Neuroimage 2005; 24: 533–8.

Bagnato F, Jeffries N, Richert ND, Stone RD, Ohayon JM, McFarland HF, et al. Evolution of T1 black holes in patients with multiple sclerosis imaged monthly for 4 years. Brain 2003; 126: 1782–9.

Barbati G, Sigismondi R, Zappasodi F, Porcaro C, Graziadio S, Valente G, et al. Functional source separation from magnetoencephalographic signals. Hum Brain Mapp 2006; 27: 925–34.

Barkhof F. The clinico-radiological paradox in multiple sclerosis revisited. Curr Opin Neurol 2002; 15: 239–45.

Bitsch A, Kuhlmann T, Stadelmann C, Lassmann H, Lucchinetti C, Bruck W. A longitudinal MRI study of histopathologically defined hypointense multiple sclerosis lesions. Ann Neurol 2001; 49: 793–6.

Brett M, Leff AP, Rorden C, Ashburner J. Spatial normalization of brain images with focal lesions using cost function masking. Neuroimage 2001; 14: 486–500.

Cader S, Cifelli A, Abu-Omar Y, Palace J, Matthews PM. Reduced brain functional reserve and altered functional connectivity in patients with multiple sclerosis. Brain 2006; 129: 527–37.

Cader S, Johansen-Berg H, Wylezinska M, Palace J, Behrens TE, Smith S, et al. Discordant white matter N-acetylasparate and diffusion MRI measures suggest that chronic metabolic dysfunction contributes to axonal pathology in multiple sclerosis. Neuroimage 2007; 36: 19–27.

Caramia MD, Cicinelli P, Paradiso C, Mariorenzi R, Zarola F, Bernardi G, et al. Excitability changes of muscular responses to magnetic brain stimulation in patients with central motor disorders. Electroencephalogr Clin Neurophysiol 1991; 81: 243–50.

Caramia MD, Palmieri MG, Desiato MT, Boffa L, Galizia P, Rossini PM, et al. Brain excitability changes in the relapsing and remitting phases of multiple sclerosis: a study with transcranial magnetic stimulation. Clin Neurophysiol 2004; 115: 956–65.

Cercignani M, Bozzali M, Iannucci G, Comi G, Filippi M. Intra-voxel and inter-voxel coherence in patients with multiple sclerosis assessed using diffusion tensor MRI. J Neurol 2002; 249: 875–83.

Cichocki A, Amari SI. Adaptive blind signal and image processing. New York: Wiley; 2002.

Cover KS, Vrenken H, Geurts JJ, van Oosten BW, Jelles B, Polman CH, et al. Multiple sclerosis patients show a highly significant decrease in alpha band interhemispheric synchronization measured using MEG. Neuroimage 2006; 29: 783–8.

Del Gratta C, Pizzella V, Tecchio F, Romani GL. Magnetoencephalography - a noninvasive brain imaging method with 1 ms time resolution. Rep Prog Phys 2001; 64: 1759–814.

De Stefano N, Narayanan S, Francis SJ, Smith S, Mortilla M, Tartaglia MC, et al. Diffuse axonal and tissue injury in patients with multiple sclerosis with low cerebral lesion load and no disability. Arch Neurol 2002; 59: 1565–71.

Engel AK, Fries P, Singer W. Dynamic predictions: oscillations and synchrony in top-down processing. Nat Rev Neurosci 2001; 2: 704–16.

Fellous JM, Houweling AR, Modi RH, Rao RP, Tiesinga PH, Sejnowski TJ. Frequency dependence of spike timing reliability in cortical pyramidal cells and interneurons. J Neurophysiol 2001; 85: 1782–7.

Filippi M, Rocca MA. MRI evidence for multiple sclerosis as a diffuse disease of the central nervous system. J Neurol 2005; 252 (Suppl 5): v16–24.

Friston KJ, Holmes AP, Poline JB, Grasby PJ, Williams SC, Frackowiak RS, et al. Analysis of fMRI time-series revisited. Neuroimage 1995; 2: 45–53.

Good CD, Johnsrude IS, Ashburner J, Henson RN, Friston KJ, Frackowiak RS. A voxel-based morphometric study of ageing in 465 normal adult human brains. Neuroimage 2001; 14: 21–36.

Gray CM, Konig P, Engel AK, Singer W. Oscillatory responses in cat visual cortex exhibit inter-columnar synchronization which reflects global stimulus properties. Nature 1989; 338: 334–7.

Hebb DO. The organization of behavior. New York: Wiley; 1949.

Horwitz B. The elusive concept of brain connectivity. Neuroimage 2003; 19: 466–70.
Horwitz B, Warner B, Fitzer J, Tagamets MA, Husain FT, Long TW. Investigating the neural basis for functional and effective connectivity. Application to fMRI. Philos Trans R Soc Lond B Biol Sci 2005; 360: 1093–108.
Kaiser J, Lutzenberger W. Human gamma-band activity: a window to cognitive processing. Neuroreport 2005; 16: 207–11.
Keegan BM, Noseworthy JH. Multiple sclerosis. Annu Rev Med 2002; 53: 285–302.
Kurtzke JF. Rating neurologic impairment in multiple sclerosis: an expanded disability status scale (EDSS). Neurology 1983; 33: 1444–52.
Leocani L, Comi G. EEG coherence in pathological conditions. J Clin Neurophysiol 1999; 16: 548–55.
Leocani L, Locatelli T, Martinelli V, Rovaris M, Falautano M, Filippi M, et al. Electroencephalographic coherence analysis in multiple sclerosis: correlation with clinical, neuropsychological, and MRI findings. J Neurol Neurosurg Psychiatry 2000; 69: 192–8.
Lezak MD. Neuropsychological assessment. New York: Oxford University Press; 1976.
Lublin FD, Reingold SC. Defining the clinical course of multiple sclerosis: results of an international survey. National Multiple Sclerosis Society (USA) Advisory Committee on clinical trials of new agents in multiple sclerosis. Neurology 1996; 46: 907–11.
Lutzenberger W, Ripper B, Busse L, Birbaumer N, Kaiser J. Dynamics of gamma-band activity during an audiospatial working memory task in humans. J Neurosci 2002; 22: 5630–8.
Matthews PM. Axonal loss and demyelation in multiple sclerosis. J Neurol Neurosurg Psychiatry 1999; 67: 708–9.
Mauguière F, Allison T, Babiloni C, Buchner H, Eisen AA, Goodin DS, et al. Somatosensory evoked potentials. The international federation of clinical neurophysiology. Electroencephalogr Clin Neurophysiol Suppl 1999; 52: 79–90.
McDonald WI, Compston A, Edan G, Goodkin D, Hartung HP, Lublin FD, et al. Recommended diagnostic criteria for multiple sclerosis: guidelines from the International Panel on the diagnosis of multiple sclerosis. Ann Neurol 2001; 50: 121–7.
Oldfield RC. The assessment and analysis of handedness: the Edinburgh inventory. Neuropsychologia 1971; 9: 97–113.
Petersen CC, Sakmann B. Functionally independent columns of rat somatosensory barrel cortex revealed with voltage-sensitive dye imaging. J Neurosci 2001; 21: 8435–46.
Reddy H, Narayanan S, Arnoutelis R, Jenkinson M, Antel J, Matthews PM, et al. Evidence for adaptive functional changes in the cerebral cortex with axonal injury from multiple sclerosis. Brain 2000; 123 (Pt 11): 2314–20.
Reich DS, Smith SA, Zackowski KM, Gordon-Lipkin EM, Jones CK, Farrell JA, et al. Multiparametric magnetic resonance imaging analysis of the corticospinal tract in multiple sclerosis. Neuroimage 2007; 38: 271–9.
Riehle A, Grammont F, Diesmann M, Grun S. Dynamical changes and temporal precision of synchronized spiking activity in monkey motor cortex during movement preparation. J Physiol Paris 2000; 94: 569–82.
Rizzolatti G, Luppino G. The cortical motor system. Neuron 2001; 31: 889–901.
Singer W. Neuronal synchrony: a versatile code for the definition of relations? Neuron 1999; 24: 49–65, 111–25.
Steriade M. Neocortical cell classes are flexible entities. Nat Rev Neurosci 2004; 5: 121–34.
Tecchio F, Graziadio S, Barbati G, Sigismondi R, Zappasodi F, Porcaro C, et al. Somatosensory dynamic gamma-band synchrony: a neural code of sensorimotor dexterity. Neuroimage 2007a; 35: 185–93.
Tecchio F, Porcaro C, Barbati G, Zappasodi F. Functional source separation and hand cortical representation for a brain-computer interface feature extraction. J Physiol 2007b; 580: 703–21.
Truyen L, van Waesberghe JH, van Walderveen MA, van Oosten BW, Polman CH, Hommes OR, et al. Accumulation of hypointense lesions ('black holes') on T1 spin-echo MRI correlates with disease progression in multiple sclerosis. Neurology 1996; 47: 1469–76.
van Waesberghe JH, Kamphorst W, De Groot CJ, van Walderveen MA, Castelijns JA, Ravid R, et al. Axonal loss in multiple sclerosis lesions: magnetic resonance imaging insights into substrates of disability. Ann Neurol 1999; 46: 747–54.
Varela F, Lachaux JP, Rodriguez E, Martinerie J. The brainweb: phase synchronization and large-scale integration. Nat Rev Neurosci 2001; 2: 229–39.
von Stein A, Chiang C, Konig P. Top-down processing mediated by interareal synchronization. Proc Natl Acad Sci USA 2000; 97: 14748–53.

Appendix I
ICC estimate

The network phase locking dynamic measure was obtained accordingly with the procedure previously applied by our group (Tecchio *et al.*, 2007). After the extraction of sources related to the activity of thumb ($FS_T(t)$) and little finger ($FS_L(t)$) neuronal network (Barbati *et al.*, 2006), the network phase locking index was obtained by the following steps:

(1) the $FS_T(t)$ and $FS_L(t)$ signals were forward–backward band pass filtered in the gamma band [$\gamma = (33–45)$ Hz] by a Butterworth filter of the second order, obtaining $FS_X^\gamma(t)$ signals, where $X = T, L$;

(2) the analytic signals of $FS_X^\gamma(t)$ were calculated:

$$a_X^\gamma(t) = FS_X^\gamma(t) + ih_X^\gamma(t) \quad (1)$$

where $h_X^\gamma(t)$ is the $FS_X^\gamma(t)$ Hilbert transform. The analytic signal was studied rather than the signal itself, to separately express amplitude and phase of FS_X, maintaining the same time resolution of the original signal;

(3) the phase $\varphi_X^\gamma(t)$ of the analytic signal is:

$$\varphi_X^\gamma(t) = \mathrm{arctg}\left[\frac{h_X^\gamma(t)}{FS_X^\gamma(t)}\right] \quad (2)$$

(4) the dynamic synchronization between the FS_T and FS_L sources was defined as:

$$\mathrm{Sync}^{\gamma X}(t) = \frac{1}{N^X}\sqrt{\left[\sum_{k=1}^{N^X}\cos(\Delta\varphi^\gamma(t_k))\right]^2 + \left[\sum_{k=1}^{N^X}\sin(\Delta\varphi^\gamma(t_k))\right]^2} \quad (3)$$

where $\Delta\varphi^\gamma(t) = \varphi_L^\gamma(t) - \varphi_T^\gamma(t)$, $t_k \in [T1, T2]$, with $T2–T1$ the intervals length between two successive stimuli, N^X is the number of considered stimuli for each finger $X = \{T, L\}$. $\mathrm{Sync}^{\gamma X}(t)$ is independent of the signal amplitudes; it is a dimensionless number varying between 0 and 1: if the two signals are strictly locked ($\Delta\varphi_X^\gamma(t) = \text{constant}$) then $\mathrm{Sync}^{\gamma X}(t)$ equals 1, whereas if $\Delta\varphi_X^\gamma(t)$ varies randomly, then $\mathrm{Sync}^{\gamma X}(t)$ tends toward zero.

(5) the phase locking index ICC was finally obtained by averaging $\mathrm{Sync}^{\gamma X}(t)$ in the time interval lasting 50 ms

centred in the time point corresponding to maximal value automatically found between 20 and 75 ms after the stimulus onset (t_{MAX}):

$$\mathrm{Sync}^{YX} = \sum_{t=t_{MAX}-25}^{t_{MAX}+25} \mathrm{Sync}^{YX}(t) \quad (4)$$

To be noted, the time-dependent behaviour of the phase locking index was obtained in the two different conditions of thumb and little finger stimulations. In conclusion, the index Sync^{YX} estimates the phase synchronization between the two finger source rhythmic activities in the gamma frequency band while stimulating each of two contra-lateral fingers (X = thumb, little finger).